2015 Indian Control Conference
Indian Institute of Technology Madras
January 5-7, 2015. Chennai, India

Multi UAV Formation Control for Target Monitoring

Sangeeta Daingade, Arpita Sinha, Aseem Borkar and Hemendra Arya

Abstract— **This paper presents a target monitoring strategy with multiple autonomous vehicles. It is assumed that the vehicles are equipped with a sensor, with which each vehicle can identify and measure bearing angle of it's neighbor vehicle and the target. Each vehicle can be assigned different pursuit gain. At equilibrium agents move along a circle with rigid polygonal formation. This formation can be changed keeping the radius same by selecting proper values of pursuit gains. Simulation results are provided to verify the theoretical results. The results developed with unicycle model have been verified with 6-DOF model and Hardware In-Loop Simulator.**

I. INTRODUCTION

In the applications like convoy protection, natural resource monitoring, geographical exploration it is required to monitor a point of interest continuously from all the directions. In such applications multi vehicle systems are found suitable due to their various advantages like reliability, robustness, scalability and better efficiency. In order to accomplish a common goal these vehicles should work in cooperation. In this paper we present a bearing angle based control strategy for multiple autonomous vehicles so as to make them move from any initial position towards the target and keep moving around it with uniform distribution.

The target or a point of interest can be better monitored if the agents are distributed around it. Circular formation is one of the best formation about the target in which all the agents move keeping constant distance from the target. Vision based strategies for achieving circular formation are discussed in [1] - [7] . Moshtagh et al. [1] have proposed a vision based control law for achieving circular formation which needs only bearing angle information of the neighbors. Each vehicle is assumed to have a vision sensor for measuring bearing angle which is a quantity defined in the local body frame. The agents finally converge to a circular formation but the point about which formation converges cannot be specified a priori. In order to enable target enclosing we should be able to achieve formations about a specific point (target). Ground vehicle tracking using multiple UAVs considering vision input is discussed in [6] where the target tracking control and coordination control are designed separately. Here the tracking control is a function of both bearing angle and range measurements whereas coordination term in the control is a nonlinear function of bearing angle only. In the paper [7], the authors have proposed a bearing angle based target monitoring strategy based on cyclic pursuit. Each agent needs only bearing angle information of one of the neighbor and that of the target. The control input is a linear function of bearing angles. It is assumed that the pursuit gain is same for all the agents and they all can see the target.

In this paper we extend the work presented in [7] with different pursuit gains. This allows us to take into account different sensing capability of visual sensors. We can obtain different formations along a circle by selecting the pursuit gains appropriately. Also this allows us to consider a case when the target is in the view of only few of the agents. We study the case when the target is stationary. The analysis has been carried out considering kinematic (Unicycle) model for each agent. The results are verified with 6-DOF model and Hardware-In-Loop Simulator (HILS). It is assumed that each vehicle can identify its neighbor vehicle and can measure bearing angle with respect to it.

The paper is organized as follows. The system model is presented in Sec II followed by the discussion about possible equilibrium formations in Sec III. Section IV gives the realistic MAV model and the details of control implementations on the autopilot. Implementation of this strategy on Hardware-In-Loop Simulator is discussed in V. Simulation results are presented in Sec VI and concluding remarks are discussed in VII.

II. PROBLEM FORMULATION

Cyclic pursuit is a simple strategy derived from the behavior of social insects. Given a set of n agents, they are numbered from 1 to n and each agent i follows its neighbor agent $i+1 \pmod n$. This results into different types of patterns depending on the model of each agent and the way each agent pursues its neighbor. This strategy and its applications has been discussed in great detail in [8] - [15]. The work presented in this paper is based on target centric cyclic pursuit strategy [7] which has been derived from the cyclic pursuit strategy to monitor a stationary target with a group of n agents. The kinematics of each agent i are represented by:

$$\dot{x}_i = V_i \cos(h_i), \quad \dot{y}_i = V_i \sin(h_i), \quad \dot{h}_i = u_i = \omega_i \qquad (1)$$

where $P_i = [x_i, y_i]^T$ represents the position of agent i and h_i represents the heading angle of the agent i. V_i and ω_i represents the linear speed and angular speed of the agent i respectively. Equation (1) can represent a point mass model of a UAV flying at a fixed altitude or a point mass model of a wheeled robot on a plane. We use a generic term "agent" to represent the aerial or ground vehicle. We assume that the agent i is moving with constant linear speed, that is V_i is constant and the motion of the agent i is controlled using the angular speed, ω_i.

The authors are with the IIT Bombay, Mumbai, India 400076,(e-mail: sangeetad@sc.iitb.ac.in ; asinha@sc.iitb.ac.in ; email: aseem.v.borkar@gmail.com; arya@aero.iitb.ac.in)

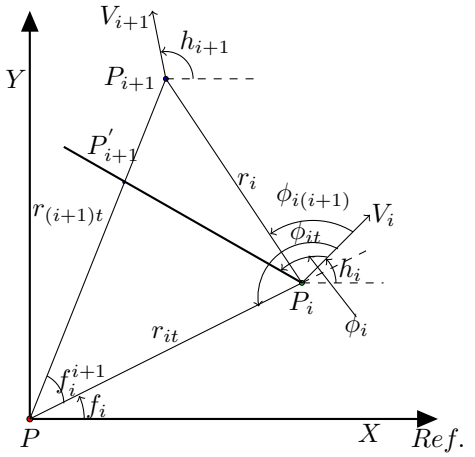

Fig. 1. Positions of the vehicles in a target centric frame

It is assumed that each vehicle is equipped with a vision sensor with which it can identify its neighbor agent as well as the target. We start with the assumption that all the agents can see the target during their entire maneuver. But later we show that it can be relaxed and the minimum requirement is that the target is in the vicinity of atleast one agent. The strategy proposed in this paper demands only bearing angle information which can be acquired easily with vision sensors. Consider Fig. 1. Point P in the Fig. 1 represents the target position. Since we are considering a stationary target, we assume a target centric reference frame. Agent i and its neighbor agent $i+1$ are located at P_i and P_{i+1} respectively. The variables in Fig. 1 are:
r_{it} – Distance between i^{th} agent and the target,
r_i – Distance between i^{th} agent and $i+1^{th}$ agent,
f_i – angle made by the vector r_{it} w.r.t reference and
f_i^{i+1} – angular separation between agent i and agent $i+1$ taken with respect to target.
ϕ_{it} – Bearing angle of agent i with respect to the target,
$\phi_{i(i+1)}$ – Bearing angle of agent i with respect to neighbor agent $i+1$ (mod n).

We modify the classical cyclic pursuit law ([10]) for target enclosing problem such that agent i, positioned at P_i, follows not only $i+1^{th}$ agent at P_{i+1} but also the target at P. Let ρ_i be a constant which decides the weight agent i gives to the target information over the information of the agent $i+1$. We call this parameter as *pursuit gain*. The parameter ρ_i can take values between 0 and 1. This weighing scheme is mathematically equivalent to following a virtual leader along the line $P_iP'_{i+1}$ with bearing angle ϕ_i. The angle ϕ_i is calculated as

$$\phi_i = (1-\rho_i)\ \phi_{it} + \rho_i\ \phi_{i(i+1)}. \tag{2}$$

We define the control input to the i^{th} agent as

$$u_i = \omega_i = k_i\phi_i \tag{3}$$

where, $k_i > 0$ is controller gain. We assume that $\phi_{it} \in [0, 2\pi)$ and $\phi_{i(i+1)} \in [0, 2\pi)$ for all time, $t \geq 0$. So $\phi_i \in [0, 2\pi)$. This condition ensures that the agents always rotate in counter clockwise direction. The kinematics (1) can be re-written in the target centric reference frame as,

$$\dot{r}_{it} = V_i\cos(h_i - f_i) \tag{4}$$

$$\begin{aligned}\dot{f}_i^{i+1} &= \dot{f}_{i+1} - \dot{f}_i \\ &= \frac{V_{i+1}\sin(h_{i+1} - f_{i+1})}{r_{(i+1)t}} - \frac{V_i\sin(h_i - f_i)}{r_{it}}\end{aligned} \tag{5}$$

$$\dot{h}_i - \dot{f}_i = \omega_i - \dot{f}_i = k_i\phi_i - \frac{V_i\sin(h_i - f_i)}{r_{it}} \tag{6}$$

Let us define the states of the system as $\mathbf{x}_{i(1)} = r_{it}$, $\mathbf{x}_{i(2)} = f_i^{i+1}$ and $\mathbf{x}_{i(3)} = h_i - f_i$ for $i = 1, 2, \cdots n$. Then we can write (4) - (6) as:

$$\dot{\mathbf{x}}_{i(1)} = V_i\cos(\mathbf{x}_{i(3)}) \tag{7a}$$

$$\dot{\mathbf{x}}_{i(2)} = \frac{V_{i+1}\sin(\mathbf{x}_{i+1(3)})}{\mathbf{x}_{i+1(1)}} - \frac{V_i\sin(\mathbf{x}_{i(3)})}{\mathbf{x}_{i(1)}} \tag{7b}$$

$$\dot{\mathbf{x}}_{i(3)} = k_i\phi_i - \frac{V_i\sin(\mathbf{x}_{i(3)})}{\mathbf{x}_{i(1)}}. \tag{7c}$$

Equation (7) gives the kinematics of i^{th} agent. In the subsequent sections, all the analysis are done based on this model.

Note 1: In practical situation, the agents will have a bound on angular speed ω_{max}, that is, $\omega_i \leq \omega_{max} \forall i$. We can take into account this constraint by imposing an upper bound on the value of k_i as, $k_i \leq k_{max}$ where $k_{max} = \frac{\omega_{max}}{2\pi}$.
Next section discusses about the possible formations at equilibrium.

III. Formation at equilibrium

In this section, we study the asymptotic behavior of the agents under the control law (3).

Theorem 1: Consider n agents with kinematics (7) and control law (3). At equilibrium the agents move on concentric circles with rigid polygonal formation.

Proof: At equilibrium $\dot{\mathbf{x}}_{i(j)} = 0$ for $i = 1, \cdots, n$ and $j = 1, 2, 3$, which implies,

$$\dot{r}_{it} = 0 \tag{8}$$

$$\dot{f}_i^{i+1} = 0 \tag{9}$$

$$\dot{h}_i - \dot{f}_i = 0 \tag{10}$$

Then from (4) - (6),

$$\mathbf{x}_{i(1)} = r_{it} = \text{constant} \tag{11}$$

$$\mathbf{x}_{i(2)} = f_i^{i+1} = \text{constant} \tag{12}$$

$$\mathbf{x}_{i(3)} = h_i - f_i = \text{constant} \tag{13}$$

From (11) we observe that the distance between the target and agent i (for all i) remains constant at equilibrium. Using (4) and (8) we can write,

$$h_i - f_i = (2m+1)\frac{\pi}{2} \tag{14}$$

where $m = 0, \pm1, \pm2, \cdots$. From (6), (10) and (14),

$$k_i\phi_i = \frac{V_i \sin(h_i - f_i)}{r_{it}} = \pm\frac{V_i}{r_{it}} \tag{15}$$

Since $k_i > 0$, $V_i > 0$ and $r_{it} \geq 0$, from (15) we get

$$k_i\phi_i = \frac{V_i}{r_{it}} \tag{16}$$

and therefore, in (14), $m = 0, \pm2, \pm4, \cdots$. Assuming $h_i \in [0, 2\pi)$ and $f_i \in [0, 2\pi)$, we get $(h_i - f_i) \in (-2\pi, 2\pi)$. Therefore $m = 0$ or $m = -2$. From geometry, $m = 0$ and $m = -2$ implies the same angle. Therefore

$$h_i - f_i = \frac{\pi}{2} \tag{17}$$

From (3) and (16),

$$\omega_i = \frac{V_i}{r_{it}}. \tag{18}$$

Since V_i and r_{it} are constant, ω_i is constant for all i. Therefore all the agents move along a circular path with the target at the center and radius r_{it}. This proves the first part of the theorem.
From equation (5), (9) and (17), we can write,

$$\frac{V_i}{r_{it}} = \frac{V_{i+1}}{r_{(i+1)t}} \tag{19}$$

Using (18) and (19), we conclude that

$$\omega_i = \omega_{i+1} \tag{20}$$

for all i. Therefore, all the agents move around the target in concentric circles with equal angular speed. So at equilibrium the agents form a rigid polygon that rotates about the target. ■

In this paper we present analysis for homogeneous agents only. The agents are assumed to be homogeneous in the sense that all of them move with equal linear speed V and equal controller gain k. As $V_i = V_{i+1}$, from (19), $r_{it} = r_{(i+1)t} = R$ for all i. Therefore at equilibrium all the agents move along a circle of radius R with the target at the center. Consider Fig. 2 which shows the position of two of the agents at equilibrium. Let P, P_i and P_{i+1} be the positions of target, agent i and agent $i+1$ respectively. From Fig. 1, $\phi_{it} = \pi - (h_i - f_i)$. Substituting the value of $h_i - f_i$ from (17),

$$\phi_{it} = \frac{\pi}{2} \tag{21}$$

for all i. Consider $\triangle P_iPP_{i+1}$. As $P_iP = P_{i+1}P = R$, $\angle PP_iP_{i+1} = \angle PP_{i+1}P_i = b_i$. Therefore $f_i^{i+1} = \pi - 2b_i$. Referring Fig. 2 and using (21), we can write $b_i = \frac{\pi}{2} - \phi_{i(i+1)}$. So

$$\phi_{i(i+1)} = \frac{f_i^{i+1}}{2}. \tag{22}$$

From (3), (18) and (20) we can write,

$$\phi_i = \phi_{i+1} = \frac{V}{kR} \tag{23}$$

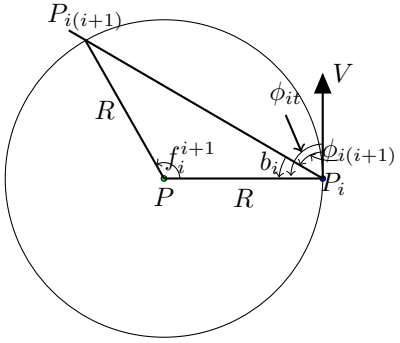

Fig. 2. Formation of agent i and agent $i+1$ at equilibrium

for all i. So using (2), (21), (22) and (23) we can write

$$(1-\rho_i)\frac{\pi}{2} + \rho_i\frac{f_i^{i+1}}{2} = (1-\rho_{i+1})\frac{\pi}{2} + \rho_{i+1}\frac{f_{i+1}^{i+2}}{2}$$

for all i. Rearranging this equation we can write

$$f_i^{i+1} = (\frac{\rho_i - \rho_1}{\rho_i})\pi + \frac{\rho_1}{\rho_i}f_1^2 \tag{24}$$

As the agents are distributed along a circle,

$$\sum_{\substack{i=1 \\ (\text{mod n})}}^{n} (f_i^{i+1}) = 2\pi d,$$

where $d = 0, \pm1, \pm2, \cdots$. Expanding this equation and substituting the value of f_i^{i+1} (from equation (24)) in terms of f_1^2, we get,

$$f_1^2 = \frac{(2\pi d - n\pi)\rho_{eq} + \pi\rho_1}{\rho_1} \tag{25}$$

where $\frac{1}{\rho_{eq}} = \frac{1}{\rho_1} + \frac{1}{\rho_2} + \cdots + \frac{1}{\rho_n}$. Using (24) and (25) we can calculate

$$f_i^{i+1} = \frac{(2\pi d - n\pi)\rho_{eq} + \pi\rho_i}{\rho_i} \tag{26}$$

for all i. This equation gives the relationship between pursuit gain ρ_i and angular separation between agent i and its neighbor. So by proper selection of pursuit gain we can get different formations. The value of ϕ_i at equilibrium can be calculated by using (2), (21), (22) and (25) as,

$$\phi_{eq} = (1 - n\rho_{eq})\frac{\pi}{2} + \rho_{eq}\pi d. \tag{27}$$

Then the equilibrium state of n agent system can be described as

$$\mathbf{x}_{i(1)} = R = \frac{V}{k\phi_{eq}} \tag{28a}$$

$$\mathbf{x}_{i(2)} = \frac{(2\pi d - n\pi)\rho_{eq} + \pi\rho_i}{\rho_i} \tag{28b}$$

$$\mathbf{x}_{i(3)} = \frac{\pi}{2}. \tag{28c}$$

Thus, at equilibrium, the agents arrange themselves in a regular formation around the target. This regular formation of n agents can be described by a regular polygon $\{n/d\}$, where $d \in \{1, 2, ..., n-1\}$. This d is reflected in equilibrium

state $\mathbf{x}_{i(2)}$ in (29b). When we consider all the agents with equal ρ that is $\rho_i = \rho_{i+1}$ for all i , it becomes a special case. The value of ρ_{eq} will be $\frac{\rho}{n}$. Also the inter-agent angular separation will be $f_i^{i+1} = f_{i+1}^{i+2} = 2\pi\frac{d}{n}$. So the equilibrium state of the system can be described as (as discussed in [7]):

$$\mathbf{x}_{i(1)} = R = \frac{V}{k\phi_{eq}} \tag{29a}$$

$$\mathbf{x}_{i(2)} = 2\pi\frac{d}{n} \tag{29b}$$

$$\mathbf{x}_{i(3)} = \frac{\pi}{2}. \tag{29c}$$

where $\phi_{eq} = (1-\rho)\frac{\pi}{2} + \rho\pi\frac{d}{n}$. Inter agent distance can be calculated as $R_{aa} = 2R\sin\left(\frac{\pi d}{n}\right)$. We can decide a switching strategy for deciding the value of ρ depending on the availability of information about the target. When we have limited information in the sense that only few of the agents are able to sense the target, the strategy can be implemented as follows:

- If all the agents are able to sense the target, set ρ to a group value ρ_g.
- If there are m number of agents which are not able to sense the target, set $\rho = 1$ for these m agents and set $\rho = \rho_g$ for remaining agents.
- If the vision sensor is able to give range measurement then, upto certain distance we can take ρ inversely proportional to the distance between the target and the agent and once they are close enough it can be set to group value ρ_g.

This algorithm is useful in the case of limited information in the sense that only few of the agents can see the target.

IV. Implementation with 6-DOF Model

In this section, we discuss implementation of proposed strategy for fixed-wing UAVs. The flight model is taken from [16], in which the wind tunnel data was obtained from National Aerospace Laboratories, Bangalore. The aerodynamic equations used are as follows:

$$\begin{aligned}
\dot{x}_e &= [u\cos\theta + (v\sin\phi + w\cos\phi)\sin\theta]\cos\psi \\
&\quad - (v\cos\phi - w\sin\phi)\sin\psi \\
\dot{y}_e &= [u\cos\theta + (v\sin\phi + w\cos\phi)\sin\theta]\sin\psi \\
&\quad + (v\cos\phi - w\sin\phi)\cos\psi \\
\dot{z}_e &= -u\sin\theta + (v\sin\phi + w\cos\phi)\cos\theta \\
\dot{\theta} &= q\cos\phi - r\sin\phi \\
\dot{\phi} &= p + (q\sin\phi + r\cos\phi)\tan\theta \\
\dot{\psi} &= \frac{(q\sin\phi + r\cos\phi)}{\cos\theta} \\
\dot{u} &= rv - qw + \frac{1}{m}f_x \\
\dot{v} &= pw - ru + \frac{1}{m}f_y \\
\dot{w} &= qu - pv + \frac{1}{m}f_z \\
\dot{p} &= \Gamma_1 pq - \Gamma_2 qr + \Gamma_3 l + \Gamma_4 n \\
\dot{q} &= \Gamma_5 pr - \Gamma_4\left(p^2 - r^2\right) + \Gamma_5 m \\
\dot{r} &= \Gamma_6 pq - \Gamma_1 qr + \Gamma_4 l + \Gamma_7 n
\end{aligned}$$

where [x_e, y_e and z_e] represents position of MAV, [u,v,w] represents velocity components of MAV in body frame. Here [ϕ, θ,ψ] and [p, q,r] are Euler angles and their rates respectively. During the flight the altitude and airspeed are held constant. Autopilot of each MAV has three control loops to regulate heading, speed and altitude using proportional-integral-derivative (PID) controllers. There are two separate autopilots for the longitudinal and lateral control. The motivation for this comes from the fact that upon linearization the longitudinal and lateral dynamics get decoupled. The longitudinal and lateral autopilots are designed using successive loop closure (refer Fig. IV). There are two inputs to the longitudinal autopilot - commanded speed (V_c) and commanded altitude (h_c). Commanded speed (V_c) is held constant. Also the commanded altitude (h_c) is held constant for simulating planner condition. Speed control is achieved by controlling throttle input. The altitude control loop generates appropriate commands for elevator defection of the MAV. Lateral autopilot command is generated using desired heading angle. The proposed algorithm is implemented in heading control. The desired heading angle or heading command χ_{i_c} is calculated using desired bearing angle as discussed in Section II (Equation 3). From flight mechanics the heading rate of MAV can be calculated as: $\dot{\chi}_i = -p\sin\theta + q\cos\theta\sin\phi + r\cos\phi\sin\theta$. We have used Runge-Kutta fourth order method to solve the system of equations with the time step of $dT = 2$ msec. It is assumed that the sensor data is available at discrete instances (one sec). The heading angle of MAV is updated at every one sec. In between two measurements it is calculated as $\chi_i = \chi_{i_m} + \sum_{t_0}^{t}\dot{\chi}_i dT$, where χ_{i_m} is the measured value of heading angle at t_0. The roll angle command ϕ_{i_c} is generated as: $\phi_{i_c} = H_{Kp}\chi_{i_e} - H_{Kd}\dot{\chi}_i$, where $\chi_{i_e} = \chi_{i_e} - \chi_{i_e}$ is heading error, H_{Kp} is proportional gain and H_{Kd} is derivative gain. Here H_{Kp} is related to controller gain k (equation 3) as $H_{Kp} = V_i k/g$ where V_i is the speed of the vehicle i and g is acceleration due to gravity. The roll command is then given to an inner PID control loop for roll control which generates appropriate commands for aileron defection as shown in Fig. IV(a).

V. Hardware in Loop Simulator

Hardware in Loop Simulator (HILS) has been used to validate the results derived in this paper. The HILS system can broadly be classified into two parts, as shown in figure 4, the simulated components and the actual hardware subsystems present in the simulation loop. Flight dynamics and sensor dynamics has been simulated as SimuLink Blocks in MATLAB on host PC. This code is run in real time on Target PC which is loaded with Real-Time Operating System RTOS xPC Target™Rapid Prototyping System v5.0. The flight simulation generates the sensor data for the On Board Computers (OBCs) in appropriate formats. The sensor information includes the GPS and IMU sentences. These sentences are serially conveyed via serial card to

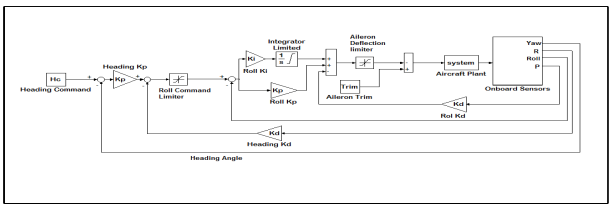

(a) Heading control

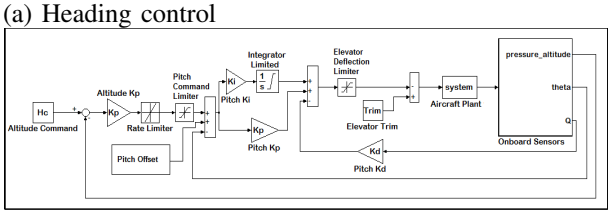

(b) Altitude control

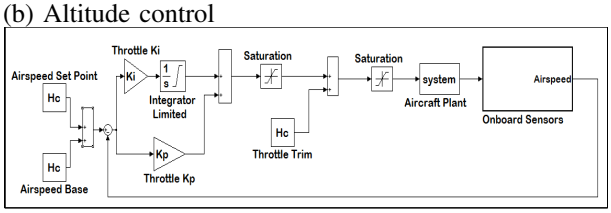

(c) Speed control

Fig. 3. MAV Autopilot Control Loops

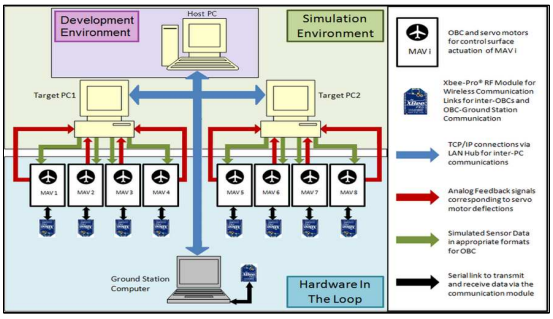

Fig. 4. Block diagram of the HILS system for for real time simulation.

the OBCs at correct baud-rates and after regular intervals. The pressure sensor data for airspeed and altitude is converted to analog voltages with proper scaling and sent to OBCs. The control algorithm resides on the OBCs which gives commands to servomotors used for surface deflection. Analog feedback from the servomotors is given as input to the flight simulation. The XBee - Pro RF module has been used for inter MAV communication as well as between MAV and ground station. All the communication links utilize the API (Application Programming Interface) mode of packet based communication. The ground station has been used for monitoring the MAV flight parameters and for tuning gains of autopilots programmed on the OBC during the real-time HILS simulations. Next section presents simulation results.

VI. Simulation Results

We considered a group of seven agents all moving with a linear speed of 15 m/sec and having controller gain $k = 0.1$. The target is stationary and is located at the origin $(0, 0)$.

Case 1: We considered agents having different values of ρ. The agents are placed at random initial positions. Fig. 5(a) shows trajectories of agents. From the Fig. 5(a) we can observe that the agents are able to capture the target but with non-uniform distributed as predicted in theory. They settle with $\{7/3\}$ formation. Table I shows different steady state parameters for different initial conditions resulting into different final formations. From the Table I it can be observed that analytical and simulation values of inter - agent angle separation and radius of the circle match exactly. Fig.5(b) shows the results in case of limited information. In this case the value of ρ is set to 1 for the agents which are not able to see the target. In this case also the desired objective of monitoring the target is achieved with nonuniform distribution. Next we considered a set of three vehicles moving

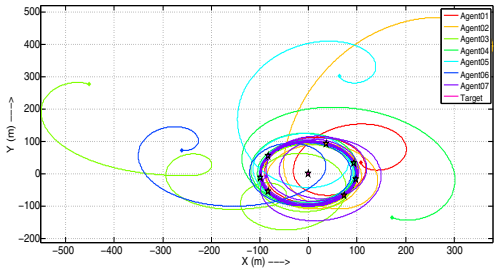

(a) $\rho = [0.1 \;\; 0.2 \;\; 0.5 \;\; 0.6 \;\; 0.4 \;\; 0.3 \;\; 0.8]$, $d = 3$

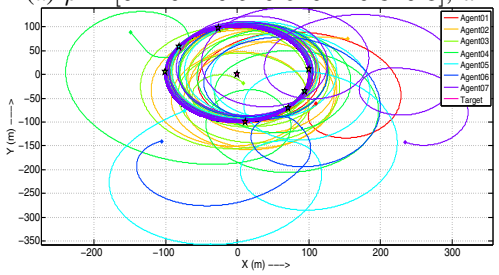

(b) $\rho = [0.1 \;\; 1 \;\; 0.5 \;\; 0.6 \;\;\; 1 \;\; 0.3 \;\; 1]$, $d = 3$

Fig. 5. Trajectories of seven agents ($\diamondsuit$ — initial position, $\star$ — final position of the agents)

with a constant speed of 15 m/sec and controller gain of 0.2. The vehicles start from random initial positions. Simulation is run for different value of ρ. Figures 6, 7 and 8 shows the trajectories of the vehicles with point mass model, 6 - DOF model and HILS respectively for $\rho = [0.9 \;\; 0.8 \;\; 0.7]$ for same initial positions. The vehicles settles along a circle whose radius is as given in Table II. The system trajectory evolution depends on the model used for representing the vehicle, number of vehicles, initial positions of the vehicles and on pursuit gain ρ. Table II shows radius of the circle and inter - agent angle at steady state. From Table II it can be observed that the final radius of the circle matches closely in all three implementations. Also theoretical values of inter-agent angles match with the simulated values.

VII. Conclusions

In this paper we proposed bearing only target centric control law for target monitoring using a group agents with different pursuit gain. The agents are modeled as planar

TABLE I

COMPARISON BETWEEN ANALYTICAL AND AND SIMULATION RESULTS FOR DIFFERENT $\rho = [0.1 \;\; 0.2 \;\; 0.5 \;\; 0.6 \;\; 0.4 \;\; 0.3 \;\; .8]$

InitialCond.	d	result	f_1^2	f_2^3	f_3^4	f_4^5	f_5^6	f_6^7	f_7^1	R
1	3	Analytical	110.09	145.05	166.02	168.35	162.52	156.69	171.26	99.35
		Simulation	110.09	145.05	166.02	168.35	162.52	156.69	171.26	99.35
2	4	Analytical	249.90	214.95	193.98	191.65	197.47	203.30	188.74	91.92
		Simulation	249.90	214.95	193.98	191.65	197.47	203.30	188.74	91.92

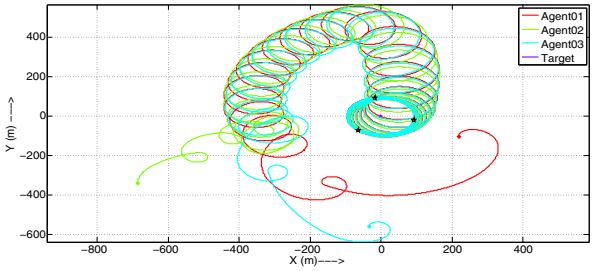

Fig. 6. Simulation result with Unicycle model

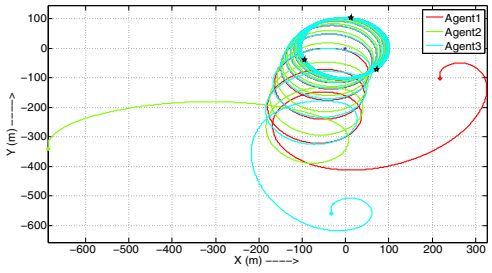

Fig. 7. Simulation result with 6-DOF MAV model

unicycles moving with constant speed. At equilibrium the agents move along concentric circles with the target at the center. When the agents are identical they move along a circle with a non-uniform distribution if they give different priority to target information and settle with uniform distribution if they all give same priority to the target information. This facilitates target monitoring even if some of the agents are not able to see the target. 6 DOF as well as HILS simulation results match with the results obtained analytically. Pursuit gain can be treated as the probability that the vehicle decides to follow its neighbor over the target. So future work would be to explore the ideas from probability theory to prove convergence results.

TABLE II

SIMULATION RESULTS WITH $\rho = [0.9 \quad 0.8 \quad 0.7]$

	Point mass	6-DOF	HILS
d	1	1	1
Radius	95.22	101.79	102.60
f_1^2	127.22	127.28	134.85
f_2^3	120.63	119.98	116.74
f_3^1	112.15	112.74	108.34

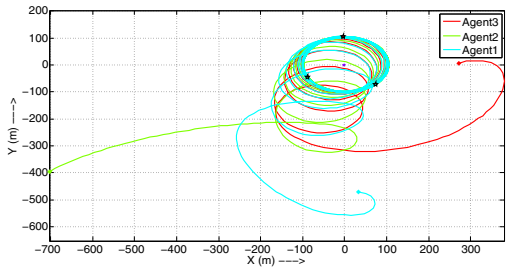

Fig. 8. Simulation result with HILS ($\diamond$: initial positions, $\star$: final positions)

REFERENCES

[1] Moshtagh, N., Michael, N., Jadbabaie, A., and Daniilidis, K., "Vision-Based, Distributed Control Laws for Motion Coordination of Nonholonomic Robots," *IEEE Transactions on Robotics*, Vol. 25(04), August 2009, pp. 851–860.

[2] Das, A., Fierro, R., Kumar, V., Ostrowski, J., Spletzer, J., and Taylor, C., "A vision based formation control framework," *IEEE Transactions on Robotics and Automation*, 2002.

[3] Mariottini, G., Morbidi, F., Prattichizzo, D., N.V. Valk, N. M., Pappas, G., and Daniilidis, K., "Vision-based localization for leaderfollower formation control," *IEEE Transactions on Robotics*, 2009.

[4] Vela, P., Betser, A., Malcolm, J., and Tannenbaum, A., "Vision-based range regulation of a leaderfollower formation," *IEEE Transactions on Control Systems Technology*, 2009.

[5] Zhao, S., Lin, F., Peng, K., Chen, B. M., and Lee, T. H., "Distributed control of angle-constrained cyclic formations using bearing-only measurements," *Systems & Control Letters 63 (2014) 1224*, 2014.

[6] Ma, L. and Hovakimyan, N., "Cooperative Target Tracking in Balanced Circular Formation: Multiple UAVs Tracking a Ground Vehicle," *Proceedings of the American Control Conference*, June 2013, pp. 5386–5391.

[7] Daingade, S. and Sinha, A., "Target Centric Cyclic Pursuit Using Bearing Angle Measurements Only," *Advances in Control and Optimization of Dynamical Systems (ACODS-2014) 03(01) 491-496*, 2014.

[8] A. Bruckstein, N. Cohen, and A. Efrat, "Ants, crickets and frogs in cyclic pursuit," *Center for Intelligence Systems,Technical Report 9105, Technion-Israel Institute of Technology, Haifa, Israel*, 1991.

[9] A. Bruckstein, "Why the ant trail look so straight and nice," *The Mathematical Intelligencer*, vol. 15(02), pp. 59–62, 1993.

[10] J. A. Marshall, M. E. Broucke, and B. A. Francis, "Formations of vehicles in cyclic pursuit," *IEEE Transaction on Automatic Control*, vol. 49(11), pp. 1963–1974, 2004.

[11] A. Sinha and D. Ghosh, "Generalization of linear cyclic pursuit with application to rendezvous of multiple autonomous agents," *IEEE Transactions on Automatic Control*, vol. 51(11), pp. 1818–1824, 2006.

[12] A. Sinha and D. Ghosh, "Generalization of nonlinear cyclic pursuit," *Automatica*, vol. 43(11), pp. 1954–1960, 2007.

[13] M. Pavone and E. Frazzoli, "Decentralized policies for geometric pattern formation and path coverage," *ASME Journal on Dynamic Systems, Measurement, and Control*, vol. 129(05), pp. 633–643, 2007.

[14] J. Ramirez, "New decentralized algorithms for spacecraft formation control based on a cyclic approach," *Ph.D. dissertation, Massachusetts Institute of Technology, Boston*, 2010.

[15] K. S. Galloway, E. W. Justh, and P. S. Krishnaprasad, "Cyclic pursuit in three dimensions," *Proceedings of the Decision and Control Conference, Atlanta, GA, USA*, pp. 7141–7146, 2010.

[16] Krishnan, D., Borkar, A. V., Shevare, P., and Arya, H., "Hardware in Loop Simulator for Cooperative Missions," *Second International Conference on Advances in Control and Optimization of Dynamical Systems*, February 2011.